Title

Biomimetic Nanoemulsions for Oxygen Delivery In Vivo.

Journal

Advanced Materials, 30(49)

Authors

Zhuang, Jia
Ying, Man
Spiekermann, Kevin
et al.

Publication Date

2018-12-01

DOI

10.1002/adma.201804693

Peer reviewed

HHS Public Access

Author manuscript

Adv Mater. Author manuscript; available in PMC 2019 December 01.

Published in final edited form as:

Adv Mater. 2018 December ; 30(49): e1804693. doi:10.1002/adma.201804693.

Biomimetic Nanoemulsions for Oxygen Delivery *In Vivo*

Jia Zhuang, **Dr. Man Ying**, **Kevin Spiekermann**, **Maya Holay**, **Yue Zhang**, **Dr. Fang Chen**, **Dr. Hua Gong**, **Joo Hee Lee**, **Dr. Weiwei Gao**, **Dr. Ronnie H. Fang**, and **Prof. Liangfang Zhang**

Department of NanoEngineering and Moores Cancer Center, University of California San Diego, La Jolla, CA 92093, U.S.A.

Abstract

Blood transfusion is oftentimes required for patients suffering from acute trauma or undergoing surgical procedures in order to help maintain the body's oxygen levels. The continued demand worldwide for blood products is expected to put significant strain on available resources and infrastructure. Unfortunately, efforts to develop viable alternatives to human red blood cells for transfusion have generally been unsuccessful. Here, we report on a hybrid natural–synthetic nanodelivery platform that combines the biocompatibility of natural RBC membrane with the oxygen carrying ability of perfluorocarbons. The resulting formulation can be stored long-term and exhibits a high capacity for oxygen delivery, helping to mitigate the effects of hypoxia *in vitro*. In an animal model of hemorrhagic shock, mice are resuscitated at an efficacy comparable to whole blood infusion. By leveraging the advantageous properties of its constituent parts, this biomimetic oxygen delivery system may have the potential to address a critical need in the clinic.

Graphical Abstract

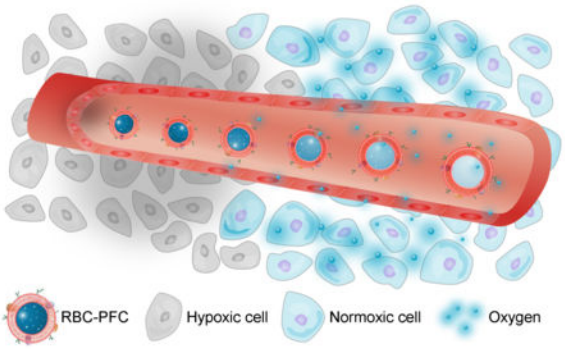

Table of content entry:

A biomimetic oxygen delivery carrier is synthesized by employing natural cell membrane as a stabilizer for perfluorocarbon nanoemulsions. The resulting formulation exhibits a high capacity for delivering oxygen and can be used to successfully resuscitate mice in an animal model of

zhang@ucsd.edu, Tel: +1-858-246-0999

Conflict of Interest

The authors declare no conflict of interest.

hemorrhagic shock. This natural–synthetic platform may eventually be used to help alleviate the impact of blood shortages in clinical settings

Keywords

biomimetic nanoparticle; oxygen delivery; blood substitute; perfluorocarbon; hemorrhagic shock

Ever since methods for the typing and storage blood were developed early in the 20th century, blood transfusions have become an essential part of modern medicine.[1] The ability of donated red blood cells (RBCs) to restore oxygen transport capacity is a life-saving measure for patients who have lost significant blood volume. The procedure is commonly employed in cases of acute trauma and during surgical procedures.[2, 3] Currently, donated RBCs, particularly those from universal donor types, are a precious resource that have a limited shelf-life under standard storage conditions, and cancellations of elective surgeries are common in times of short supply.[4] Although efforts to lessen blood utilization by doctors and supply chain management improvements can help to reduce shortages,[5, 6] these methods alone are not expected to fully address the issue. As such, significant efforts have also been placed on finding alternative strategies to help reduce the demand for timely human donations.[7–10] Promising candidates have included platforms based on hemoglobin and perfluorocarbons (PFCs), although both have been met with significant challenges in terms of clinical translation. Currently, Fluosol-DA represents the only synthetic oxygen carrier to have been approved by the United States Food and Drug Administration; however, it was taken off the market 5 years after approval in 1989 due to difficulties in its storage and use.[11]

PFC emulsions are attractive for oxygen delivery applications due to their inertness, inherent ability to solubilize gases, and small size.[12–15] As a result of their chemical structure, PFCs are highly hydrophobic and lowly reactive, giving them the capability to dissolve large amounts of gases such as oxygen and carbon dioxide. Compared with water, many PFCs have nearly 20 times the capacity for oxygen dissolution. As this is a physical process, a larger proportion of the carried oxygen is generally available for release to the tissues when compared with hemoglobin, which follows a sigmoidal dissociation curve.[16] Further, PFC emulsions can be fabricated at the nanoscale,[17, 18] and this small size enables them to deliver oxygen even to the smallest of capillaries. Despite their advantages, PFC-based platforms generally have not experienced much clinical success, which can largely be attributed to issues such as difficulty of storage and adverse immune reactions.[9]

Here, we sought to evaluate the feasibility of generating a biomimetic PFC nanoformulation for use as an oxygen delivery vehicle (Figure 1a). The use of cell membrane coatings is an emerging nanotechnology that has been shown to widely enhance the ability of synthetic nanomaterials to interface with complex biological environments *in vivo*.[19–22] Cell membrane-coated nanoparticles have been successfully fabricated from a wide range of cell types, and each of them exhibits unique properties that can be leveraged for a variety of applications.[23–31] In particular, the use of RBC coatings has demonstrated exceptional utility for improving biocompatibility and reducing immunogenicity.[32–34] In the present

work, RBC membrane is used to stabilize PFC nanoemulsions (denoted ‘RBC-PFCs’), and the oxygen carrying capacity of the resulting formulation is evaluated. The ability of the RBC-PFCs to reverse hypoxia-induced effects both *in vitro* and in an animal model of hemorrhagic shock are then demonstrated.

First, it was necessary to demonstrate that cell membrane material could be used to facilitate the formation of stable PFC nanoemulsions. For this purpose, the membrane derived from RBCs was chosen, given its previously demonstrated ability to enhance circulation, prevent cellular uptake, and improve immunocompatibility.[24, 32, 33, 35] Perfluorooctyl bromide, which readily forms nanoemulsions,[36–38] was chosen as the model PFC given its widespread study and use as an oxygen carrier.[16] Various amounts of the PFC were mixed with purified RBC membrane and emulsified by sonication (Figure 1b). It was found that, as the input of the PFC increased, the size of the emulsions also increased, with the final size growing dramatically to above 200 nm at PFC to membrane protein ratios greater than 12.5 μL/mg. At this threshold ratio, it was further shown that the size of the formulation decreased with increasing emulsification times, with the final size reaching below 200 nm after approximately 60 s (Figure 1c). With further input of energy beyond 2 min, there was a much less pronounced reduction in the final size of the RBC-PFCs. Subsequent studies were conducted using RBC-PFCs fabricated at a PFC to protein ratio of 12.5 μL/mg and with 3 min of sonication.

To confirm that the RBC membrane material was successfully associated with the PFC, the RBC membrane was labeled with a lipophilic far-red fluorescent dye that visually appears blue in color. When the RBC-PFCs were centrifuged at a low speed, significant blue color was observed in the pellet (Figure 1d). In contrast, RBC vesicles alone centrifuged at the same speed did not pellet, leaving all the blue color in the supernatant. Additionally, when PFC was emulsified, followed by mixing with RBC vesicles, significantly less blue color was observed in the pellet, indicating that the spontaneous association between the two components was limited. Overall, this experiment provided a strong indication that, in the final RBC-PFC formulation, the RBC and PFC components were successfully associated together. This was further confirmed by confocal fluorescence microscopy, where a green fluorescent dye was used to label the PFC core in addition to the far-red dye that was used to label the RBC membrane. In this case, significant colocalization of the two fluorescent channels was observed, providing another qualitative indication of a close association between the RBC membrane and PFC components (Figure 1e). In total, the data indicated that biological membrane could be used to directly facilitate the emulsification of the PFC.

We next sought to characterize the physicochemical properties of the optimized RBC-PFC formulation. Dynamic light scattering measurements revealed that the final nanoemulsions were approximately 170 nm in diameter (Figure 2a). This was significantly smaller than PFC emulsified alone in the absence of RBC membrane, which measured almost 400 nm after synthesis, and it was slightly larger than sonicated RBC membrane, which produced vesicles approximately 150 nm in diameter. The sizing data highlights to role of the RBC membrane as a stabilizer of the PFC during the emulsification process, enabling the formation of smaller sized droplets. Additionally, the surface zeta potential of RBC-PFCs was shown to be near identical to that of RBC vesicles alone, suggesting that the membrane

had masked the highly negative zeta potential of the PFC cores (Figure 2b). These results were consistent with previous works where cell membrane was used to coat negatively charged nanoparticulate cores.[25, 39] Fluorine-19 nuclear magnetic resonance (^{19}F NMR) was then used to determine the amount of PFC that was retained in the final nanoformulation. RBC-PFCs were spiked with a known concentration of perfluoro-15-crown-5-ether and subjected to ^{19}F NMR spectroscopy (Figure 2c). By comparing the integrated area for each characteristic peak and taking into consideration the number of fluorine groups contributing to each group, it was calculated that approximately 62% of the inputted PFC was retained after fabrication of the RBC-PFCs.

In order to test if the RBC-PFC formulation was suitable for long-term storage, its stability in solution was assessed over time (Figure 2d). The nanoemulsions exhibited little increase in size over the course of 96 days, staying at around 200 nm for the entire duration. In contrast, the non-stabilized PFC emulsions quickly grew after synthesis, reaching nearly 1 μm within 1 day. This data further confirmed that the RBC membrane could serve as a good stabilizer for the PFC and suggested that the two components remained strongly associated with each other over time. To evaluate oxygen delivery capacity, 20 mL of water was first deoxygenated by nitrogen purging. Subsequently, various samples were injected into the closed system and the dissolved oxygen (DO) levels were monitored over time (Figure 2e). The RBC-PFCs exhibited an exceptional ability to introduce oxygen into the deoxygenated water, elevating DO levels to near 2.0 mg/L, whereas the addition of oxygenated water alone resulted in a level of approximately 0.6 mg/L. The formulation also outperformed PFC emulsions without membrane stabilization; the extra oxygen carrying capacity of the RBC-PFC formulation could likely be attributed to residual membrane-associated hemoglobin present on the RBC vesicles, which alone were slightly better than oxygenated water. Notably, the RBC-PFC formulation also outperformed whole RBCs when normalized to the same amount of membrane. To evaluate the translational potential of the platform, RBC-PFCs were fabricated using both in-dated and just-expired human RBCs obtained from a local blood bank (Figure 2f). It was found that the dissolved oxygen kinetics between the two formulations were identical. Further, the RBC-PFC nanoemulsions were evaluated after 1 week of storage at either 4 °C or room temperature, and the performance of both samples was nearly identical to freshly made RBC-PFC.

After characterization of the RBC-PFC formulation, we then sought to evaluate the ability of the nanoemulsions to mitigate the effects of hypoxia on cells *in vitro*. First, the safety of the formulation was evaluated on Neuro2a, a murine neuroblastoma cell line, which has previously been used to study the effects of hypoxia.[40] Across the concentrations tested, the RBC-PFC formulation had no harmful impact on cell viability (Figure 3a). As PFCs are known to exert immunological effects on macrophages,[41] the impact of RBC-PFC on murine J774 macrophages was evaluated (Figure 3b). Whereas culture with non-stabilized PFC emulsions significantly elevated the level of interleukin 1 beta (IL-1β), an indicator of macrophage activation,[42] culture with RBC-PFC resulted in cytokine levels consistent with baseline. Next, the ability of the RBC-PFC formulation to rescue cells from hypoxic conditions was evaluated. Neuro2a cells were cultured under hypoxia for varying amounts of time, followed by addition of RBC-PFCs. The cells were then cultured for another 24 h, again under hypoxic conditions, and the effects on cell viability were assessed (Figure 3c).

With 6 h of hypoxia induction, the nanoformulation was highly effective in preserving cell viability, with near full efficacy across the concentrations tested. Even after 18 h of induction, full preservation of viability could be achieved when employing RBC-PFCs at high concentrations. After 24 h of hypoxia induction, full viability could no longer be reached, even at the highest amount of nanoemulsions tested, although it was observed that viability trended upwards with increasing concentration.

To further study the impact of RBC-PFCs on cells *in vitro*, the expression of hypoxia-inducible factor 1-alpha (HIF1α), a characteristic intracellular marker of hypoxia,[43] was evaluated by western blotting analysis (Figure 3d). When employing 18 h of hypoxia induction, expression of HIF1α could easily be detected in untreated cells, whereas addition of the RBC-PFCs completely abrogated expression of the protein. The western blotting results of cells treated with the nanoformulation were consistent with those from cells cultured under normoxic conditions. The impact of the RBC-PFC formulation could also be readily visualized under brightfield microscopy, with the treated cells looking healthier and denser when compared with untreated cells (Figure 3e). This was also seen when staining cells with a commercial detection reagent, which could be used to fluorescently visualize hypoxic cells (Figure 3f). Significant fluorescent signal was observed in cells after being subjected to hypoxia, whereas treatment with RBC-PFCs resulted in the absence of signal. These effects were even more pronounced following an 18 h hypoxia induction period, where the nanoemulsions were able to reverse the effects of exposure to low oxygen levels (Figure 3g,h).

Upon successfully confirming the activity of the RBC-PFC formulation *in vitro*, an animal model of hemorrhagic shock was used to evaluate *in vivo* oxygen delivery efficacy.[44] To establish this model, mice were anesthetized, and a femoral artery was cannulated. Blood was then slowly withdrawn from the cannulated artery using a syringe pump such that the mean arterial pressure (MAP) reached a critical level of 35 mmHg. After allowing the mice to stabilize for a period of 10 min, various resuscitation fluids were administered via syringe pump, and MAP was monitored over time (Figure 4a,b). When reinfused with the as withdrawn whole blood, the MAP value quickly recovered back to baseline levels, which was the expected outcome. This was also the case for the RBC-PFC formulation; the kinetics were slightly delayed compared with whole blood, but the MAP settled at the same final value of approximately 75 mmHg. In contrast, both the PFC emulsion and RBC vesicle controls performed similarly to Ringer's lactate solution, which served as a negative control. For these groups, the MAP values stabilized at just over 45 mmHg, which was still near the critical induction value. The enhanced resuscitation ability of the RBC-PFC formulation may result from its increased oxygen carrying capacity, as well as from the improved stability characteristics bestowed by the cell membrane,[24] which should enhance RBC-PFC blood residence compared with the non-stabilized PFC emulsions.

Finally, we sought to evaluate the *in vivo* biodistribution of the RBC-PFCs and assess their safety. To study the organ level distribution, the nanoemulsions were labeled with a fluorescent dye, followed by intravenous administration through the tail vein. At set time points, the mice were then euthanized, and the major organs were analyzed for their fluorescent signal (Figure 4c). From the results, it could be seen that a majority of the RBC-

PFCs was found in the liver, with significant amounts also present in the spleen and the blood at all of the time points studied. This pattern of distribution is consistent with other cell membrane-derived formulations.[24] To evaluate safety, a high bolus dose of RBC-PFCs was administered intravenously, followed by tracking of serum IL-1β levels (Figure 4d). Whereas non-stabilized PFC emulsions elicited a significant spike at 12 h post-administration, cytokine levels after injection of RBC-PFC nanoemulsions remained at baseline levels. We further performed a comprehensive analysis of blood chemistry and major blood cell populations 24 h after RBC-PFC administration (Figure 4e,f). Compared to mice administered with vehicle only, no statistical difference was observed in any of the parameters that were studied. Subsequently, the major organs were collected and subjected to histological sectioning (Figure 4g). Analysis after hematoxylin and eosin (H&E) staining revealed normal appearance in all the organs studied, including the liver, spleen, heart, lungs, and kidneys.

In conclusion, we have demonstrated the successful fabrication of a natural–synthetic oxygen delivery vehicle consisting of PFC stabilized by cell-derived membrane. The resulting nanoformulation was shown to be highly stable over time and had improved oxygen carrying capacity compared with whole RBCs. Notably, the RBC-PFC formulation was able to attenuate the effects of hypoxia *in vitro* and was able to fully resuscitate mice in a model of hemorrhagic shock. The platform incorporates the advantages of both component parts, combining the high oxygen carrying capacity of the synthetic PFC with the biocompatibility of the natural cell membrane. It can be envisioned that RBC-PFC fabrication, a facile process that converts RBCs into stable semi-synthetic nanoparticulates, can be employed in the future as a means of prolonging the usefulness of perishable human donations. RBC-PFCs can be synthesized from just-expired RBCs in times of surplus and banked in long-term storage for use during periods of high demand, which would greatly simplify the logistics of blood supply management. As a potent oxygen carrier, these biomimetic nanoemulsions could ultimately help to address an area of significant need in the clinic.

Experimental Section

Preparation and Characterization of RBC-PFCs.

All animal experiments followed protocols that were reviewed, approved, and performed under the regulatory supervision of the University of California San Diego's Institutional Animal Care and Use Committee (IACUC). Fresh RBCs were purified from whole blood collected from male CD-1 mice (Envigo), and membrane ghosts were obtained by hypotonic lysis.[24] The RBC membrane was suspended at a final protein concentration of 2 mg/mL for further use. To prepare RBC-PFCs, varying volumes of the PFC perfluorooctyl bromide (Sigma Aldrich) were mixed with 2 mL of RBC membrane solution, followed by emulsification on ice using a Fisher Scientific 150E Digital Sonic Dismembrator for increasing amounts of time with an on/off interval of 2 s/1 s. The resulting RBC-PFCs were centrifuged at 600*g* for 5 min to remove excess membrane vesicles, followed by resuspension in water or the appropriate media. Size and zeta potential measurements were conducted by dynamic light scattering using a Malvern Instruments Zetasizer Nano ZS.

Following the optimization experiments, the final RBC-PFC formulation was fabricated at a ratio of 12.5 μL PFC per 1 mg of RBC membrane protein with 3 min of emulsification. All stated RBC-PFC concentrations are expressed in terms of the protein content of the formulation. RBC vesicle and PFC emulsion controls were fabricated by sonicating the individual components for 3 min. For the stability study, samples were stored at room temperature, and size was measured periodically.

Imaging of RBC-PFCs.

To label the RBC membrane with 1,1'-dioctadecyl-3,3,3',3'-tetramethylindodicarbocyanine perchlorate (DiD, excitation/emission = 644/665 nm; Invitrogen), the dye was added to the membrane solution at a final concentration of 10 μg/mL. For dye staining of the PFC core, BODIPY FL iodoacetamide (excitation/emission = 503/512 nm; Invitrogen) was modified with 3,3,4,4,5,5,6,6,7,7,8,8,9,9,10,10,10-heptadecafluoro-1-decanethiol (Sigma Aldrich) using a previously reported approach.[45] The resulting conjugate was then dissolved at 0.2 mg/mL in the PFC. For fluorescent imaging of the RBC-PFCs, dual-labelled samples were immobilized on glass slides with Tissue-Tek OCT compound (Sakura Finetek) and visualized using an Olympus FV1000 confocal microscope.

PFC Loading Quantification.

In order to quantify the loading of PFC into the final RBC-PFC formulation, Triton X-100 (Sigma Aldrich) was added at a final ratio of 0.5% to disrupt the RBC membrane. The PFC was then extracted by mixing the lysed RBC-PFC solution with an equal volume of deuterated chloroform (Sigma Aldrich). As an internal standard, 2 μL of perfluoro-15-crown-5-ether (Sigma Aldrich) was added to 1 mL of the chloroform fraction. The sample was then subject to ^{19}F-NMR on a JEOL ECA 500 NMR spectrometer. Data analysis was performed using Mestrelab Research MestReNova software.

Dissolved Oxygen Kinetics.

A measurement apparatus was built by covering a 100 mL beaker with a foam cap, which was sealed in place using Parafilm M (Bemis). Three holes were cut into the foam cap in order to accommodate a temperature probe, an oxygen probe, and a glass pipette for nitrogen purging. Before the start of each experiment, 20 mL of water was added into the beaker, equilibrated to 37 °C, and purged with nitrogen to remove dissolved oxygen. Then, 2 mL of RBC-PFCs at 2 mg/mL was injected into the system 30 s after nitrogen flow shutdown, and the dissolved oxygen values were monitored using a Hanna Instruments edge dedicated dissolved oxygen meter. RBC vesicle and PFC emulsion controls were employed at concentrations equivalent to the RBC-PFC formulation. The whole RBC sample was used at an RBC content with equivalent membrane protein compared with the RBC-PFC samples. In-dated and outdated (2 days post-expiration) human O-positive RBCs were obtained from the San Diego Blood Bank.

In Vitro Toxicity and Hypoxia Studies.

Murine neuroblastoma Neuro2a cells (CCL-131; American Type Culture Collection) and J774 macrophages (TIB-67; American Type Culture Collection) were maintained in

Dulbecco's modified eagle medium (HyClone) supplemented with 10% fetal bovine serum (HyClone) and 1% penicillin-streptomycin (Gibco). To assess the toxicity of RBC-PFCs, Neuro2a cells were seeded in 96-well plates at 1×10^4 cells per well. The cells were then incubated under normoxic conditions (20% O_2/5% CO_2/75% N_2) in a Thermo Scientific Heracell 150i incubator with RBC-PFCs at various concentrations. After 24 h, cell viability was quantified using a CellTiter AQ_{ueous} One Solution cell proliferation assay (Promega) following the manufacturer's instructions. To evaluate the potential immunological impact of the nanoformulation, RBC-PFC was incubated with J774 cells at a concentration of 4 mg/mL. A PFC emulsion control was employed at an equivalent concentration. At 24 h, the culture medium was collected, and cytokine concentrations were assessed using a mouse IL-1β ELISA kit (Biolegend) per the manufacturer's instructions.

For the hypoxia treatment study, Neuro2a cells were cultured under hypoxic conditions (1% O_2/5% CO_2/94% N_2) in a Thermo Scientific Forma Series 3 WJ incubator for various induction periods. Afterwards, the media was replaced with fresh media containing various RBC-PFC concentrations and the cells were kept under hypoxic conditions for another 24 h before assessing cell viability. For the imaging studies, Image-iT Green hypoxia reagent (Invitrogen) was added to the cells at a final concentration of 5 μM for 30 min before washing the cells with fresh media. The cells were then subject to various hypoxia induction periods before the media was replaced with fresh media containing RBC-PFCs at 4 mg/mL. Cells were incubated for another 6 h and 24 h under hypoxic conditions before imaging under fluorescence and brightfield microscopy, respectively, using a Thermo Fisher Scientific EVOS FL cell imaging system. The control normoxia group was cultured under normoxic conditions for the duration of the experiment.

To assess the levels of HIF1α, Neuro2a cells were seeded at 5×10^5 cells per well in 6-well plates. Cells were incubated under hypoxic conditions for 18 h, after which the media was replaced with fresh media, either with or without 4 mg/mL of RBC-PFCs. The cells were then cultured for another 24 h under hypoxic conditions. The normoxia group stayed under normoxic conditions for the duration of the experiment. Afterwards, the cells were lysed on ice with RIPA buffer (Sigma Aldrich), supplemented with 1% 0.5 M ethylenediaminetetraacetic acid (Invitrogen) and 1% of a protease inhibitor cocktail (Sigma Aldrich). Lysed cells were then scraped off the wells and centrifuged at 14,000*g*, after which the supernatant was collected. Protein concentrations were normalized to 1 mg/mL. The samples were prepared using NuPAGE 4× lithium dodecyl sulfate sample loading buffer (Invitrogen) and then run on 12-well Bolt 4–12% bis-tris minigels (Invitrogen) in MOPS running buffer (Invitrogen). After transferring to 0.45 μm nitrocellulose membrane (Pierce) in Bolt transfer buffer (Invitrogen) at 10 V for 60 min, the membranes were blocked with 5% bovine serum albumin (Sigma Aldrich) in phosphate buffered saline (PBS, Mediatech) with 0.05% Tween 20 (National Scientific). The blots were then incubated with anti-HIF1α (28b; Santa Cruz Biotechnology), followed by the appropriate horse radish peroxidase-conjugated secondary antibody (Biolegend). ECL western blotting substrate (Pierce) and a Mini-Medical/90 developer (ImageWorks) were used to develop and image the blots.

In Vivo Hemorrhagic Shock Treatment.

To evaluate efficacy in a hemorrhagic shock model, 6-week-old male CD-1 mice were intraperitoneally administered with a cocktail of ketamine (Pfizer) at 100 mg/kg and xylazine (Lloyd Laboratories) at 20 mg/kg. Anesthesia was maintained for the entire surgical procedure and the mice were kept on a 37 °C heat pad. A 0.5 cm incision parallel to where the right femoral artery runs in the groin area between the abdomen and thigh was made using a small surgical scissor. The femoral artery was carefully isolated, and a small incision was then cut into the artery so that PE-10 tubing (Braintree Scientific) primed with 0.3% heparin (Sigma Aldrich) in PBS could be inserted as the cannula. The tubing was connected to a Digi-Med BPA-400 blood pressure analyzer for the continuous monitoring of MAP. The left femoral artery was cannulated in a similar fashion and connected to a Kent Scientific GenieTouch syringe pump to perform the hemorrhagic shock and resuscitation procedure. To induce hemorrhage, blood was steadily withdrawn from the left femoral artery at a constant rate of 0.1 mL/min until the MAP reached 35 mmHg, after which the mice were allowed to stabilize for 10 min. For resuscitation, 1 mL of RBC-PFCs at 2 mg/mL was infused into the left femoral artery at a constant speed of 0.1 mL/min. Ringer's lactate (Fisher Scientific) was used as a negative control, and the withdrawn whole blood was reinfused as a positive control. RBC vesicles and PFC emulsions were used at concentrations equivalent to the RBC-PFC formulation. Solutions that were not isotonic were adjusted to the appropriate osmolarity using concentrated sucrose (Sigma Aldrich). The mice were monitored for another 20 min after completion of the infusion. MAP values were recorded for the duration of the study, and the mice were euthanized immediately afterwards.

RBC-PFC In Vivo Biodistribution and Safety.

To study the biodistribution, DiD-labeled RBC-PFCs with 1.6 mg of protein content was administered via the tail vein. At 1, 4, and 24 h, mice were euthanized and their major organs, including the liver, spleen, heart, lungs, kidneys, and blood were collected and weighed. The organs were then homogenized in 1 mL of PBS using a Biospec Mini-Beadbeater-16. Fluorescence was read using a Tecan Infinite M200 plate reader. Total weight of blood was estimated as 6% of mouse body weight. To assess serum cytokine levels, RBC-PFCs with 4 mg of protein content, or an equivalent amount of PFC emulsions, were intravenously administered. At 4, 12, and 24 h after administration, blood was sampled by submandibular puncture, and cytokine levels were assessed using a mouse IL-1β ELISA kit per the manufacturer's instructions. For the other safety studies, RBC-PFCs with 4 mg of protein content was administered intravenously, and after 24 h the blood and major organs were collected for analysis. For the comprehensive metabolic panel, aliquots of blood were allowed to coagulate, and the serum was collected by centrifugation. For the blood counts, blood was collected into potassium-EDTA collection tubes (Sarstedt). Lab tests were performed by the UC San Diego Animal Care Program Diagnostic Services Laboratory. For histological analysis, the major organs were sectioned and stained with hematoxylin and eosin (Leica Biosystems), followed by imaging using a Hamamatsu Nanozoomer 2.0-HT slide scanning system.

Acknowledgements

This work is supported by the National Institutes of Health under Award Number R01CA200574.

References

[1]. Giangrande PL, Br. J. Haematol 2000, 110, 758. [PubMed: 11054057]

[2]. Goodnough LT, Brecher ME, Kanter MH, AuBuchon JP, Engl N J. Med 1999, 340, 438.

[3]. Napolitano LM, Kurek S, Luchette FA, Corwin HL, Barie PS, Tisherman SA, Hebert PC, Anderson GL, Bard MR, Bromberg W, Chiu WC, Cipolle MD, Clancy KD, Diebel L, Hoff WS, Hughes KM, Munshi I, Nayduch D, Sandhu R, Yelon JA, Crit. Care. Med 2009, 37, 3124. [PubMed: 19773646]

[4]. Goodnough LT, Shander A, Anesthesiology 2012, 116, 1367. [PubMed: 22487863]

[5]. Tinmouth A, Macdougall L, Fergusson D, Amin M, Graham ID, Hebert PC, Wilson K, Arch. Intern. Med 2005, 165, 845. [PubMed: 15851633]

[6]. Belien J, Force H, Eur. J. Oper. Res2012, 217, 1.

[7]. Buehler PW, D'Agnillo F, Schaer DJ, Trends Mol. Med 2010, 16, 447. [PubMed: 20708968]

[8]. Chen JY, Scerbo M, Kramer G, Clinics (Sao Paulo) 2009, 64, 803. [PubMed: 19690667]

[9]. Castro CI, Briceno JC, Artif. Organs 2010, 34, 622. [PubMed: 20698841]

[10]. Henkel-Honke T, Oleck M, AANA J 2007, 75, 205.

[11]. Spence RK, Norcross ED, Costabile J, Mccoy S, Cernaianu AC, Alexander JB, Pello MJ, Atabek U, Camishion RC, Artif. Cells Blood Substit. Biotechnol 1994, 22, 955.

[12]. Riess JG, Artif. Cells Blood Substit. Biotechnol 2006, 34, 567.

[13]. Lowe KC, Comp. Biochem. Phys. A 1987, 87, 825.

[14]. Lowe KC, Tissue Eng 2003, 9, 389. [PubMed: 12857407]

[15]. Riess JG, Artif. Cells Blood Substit. Biotechnol 2005, 33, 47.

[16]. Lowe KC, J. Mater. Chem 2006, 16, 4189.

[17]. Winter PM, Cai K, Caruthers SD, Wickline SA, Lanza GM, Expert Rev. Med. Devices 2007, 4, 137. [PubMed: 17359221]

[18]. Cheng Y, Cheng H, Jiang C, Qiu X, Wang K, Huan W, Yuan A, Wu J, Hu Y, Nat. Commun. 2015, 6, 8785. [PubMed: 26525216]

[19]. Fang RH, Jiang Y, Fang JC, Zhang L, Biomaterials 2017, 128, 69. [PubMed: 28292726]

[20]. Fang RH, Kroll AV, Gao W, Zhang L, Adv. Mater 2018, 30, 1706759.

[21]. Kroll AV, Fang RH, Zhang L, Bioconjug. Chem 2017, 28, 23. [PubMed: 27798829]

[22]. Dehaini D, Wei X, Fang RH, Masson S, Angsantikul P, Luk BT, Zhang Y, Ying M, Jiang Y, Kroll AV, Gao W, Zhang L, Adv. Mater 2017, 29, 1606209.

[23]. Hu CM, Fang RH, Wang KC, Luk BT, Thamphiwatana S, Dehaini D, Nguyen P, Angsantikul P, Wen CH, Kroll AV, Carpenter C, Ramesh M, Qu V, Patel SH, Zhu J, Shi W, Hofman FM, Chen TC, Gao W, Zhang K, Chien S, Zhang L, Nature 2015, 526, 118. [PubMed: 26374997]

[24]. Hu CM, Zhang L, Aryal S, Cheung C, Fang RH, Zhang L, Proc. Natl. Acad. Sci. USA 2011, 108, 10980. [PubMed: 21690347]

[25]. Fang RH, Hu CM, Luk BT, Gao W, Copp JA, Tai Y, O'Connor DE, Zhang L, Nano Lett 2014, 14, 2181. [PubMed: 24673373]

[26]. Thamphiwatana S, Angsantikul P, Escajadillo T, Zhang Q, Olson J, Luk BT, Zhang S, Fang RH, Gao W, Nizet V, Zhang L, Proc. Natl. Acad. Sci. USA 2017, 114, 11488. [PubMed: 29073076]

[27]. Hu CM, Fang RH, Copp J, Luk BT, Zhang L, Nat. Nanotechnol 2013, 8, 336. [PubMed: 23584215]

[28]. Hu CM, Fang RH, Luk BT, Zhang L, Nat. Nanotechnol 2013, 8, 933. [PubMed: 24292514]

[29]. Gao M, Liang C, Song X, Chen Q, Jin Q, Wang C, Liu Z, Adv. Mater 2017, 29, 1701429.

[30]. Wei X, Gao J, Wang F, Ying M, Angsantikul P, Kroll AV, Zhou J, Gao W, Lu W, Fang RH, Zhang L, Adv. Mater 2017, 29, 1701644.

[31]. Kroll AV, Fang RH, Jiang Y, Zhou J, Wei X, Yu CL, Gao J, Luk BT, Dehaini D, Gao W, Zhang L, Adv. Mater 2017, 29, 1703969.

[32]. Luk BT, Fang RH, Hu CMJ, Copp JA, Thamphiwatana S, Dehaini D, Gao WW, Zhang K, Li SL, Zhang LF, Theranostics 2016, 6, 1004. [PubMed: 27217833]

[33]. Rao L, Bu LL, Xu JH, Cai B, Yu GT, Yu XL, He ZB, Huang QQ, Li A, Guo SS, Zhang WF, Liu W, Sun ZJ, Wang H, Wang TH, Zhao XZ, Small 2015, 11, 6225. [PubMed: 26488923]

[34]. Gao W, Hu CM, Fang RH, Luk BT, Su J, Zhang L, Adv. Mater. 2013, 25, 3549. [PubMed: 23712782]

[35]. Hu CMJ, Fang RH, Luk BT, Chen KNH, Carpenter C, Gao WW, Zhang K, Zhang LF, Nanoscale 2013, 5, 2664. [PubMed: 23462967]

[36]. Stevens TK, Ramirez RM, Pines A, J. Am. Chem. Soc 2013, 135, 9576. [PubMed: 23742228]

[37]. Lim YT, Noh YW, Kwon JN, Chung BH, Chem. Commun. (Camb) 2009, 6952. [PubMed: 19904358]

[38]. Giraudeau C, Djemai B, Ghaly MA, Boumezbeur F, Meriaux S, Robert P, Port M, Robic C, Le Bihan D, Lethimonnier F, Valette J, NMR Biomed 2012, 25, 654. [PubMed: 21953998]

[39]. Copp JA, Fang RH, Luk BT, Hu CMJ, Gao WW, Zhang K, Zhang LF, Proc. Natl. Acad. Sci. USA 2014, 111, 13481. [PubMed: 25197051]

[40]. Liu XW, Zi Y, Liu YE, Zhang YB, Xiang LB, Hou MX, Neurosci. Lett 2015, 595, 74. [PubMed: 25864781]

[41]. Cohn CS, Cushing MM, Crit. Care Clin 2009, 25, 399. [PubMed: 19341916]

[42]. Lopez-Castejon G, Brough D, Cytokine Growth Factor Rev 2011, 22, 189. [PubMed: 22019906]

[43]. Ziello JE, Jovin IS, Huang Y, Yale J Biol. Med 2007, 80, 51.

[44]. Wang Y, Wang LL, Yu WL, Gao DW, You GX, Li PL, Zhang S, Zhang J, Hu T, Zhao L, Zhou H, Biotechnol. Progr 2017, 33, 252.

[45]. Laudien J, Naglav D, Grobeta-Heitfeld C, Ferenz KB, de Groot H, Mayer C, Schulz S, Schnepf A, Kirsch M, Microencapsul J 2014, 31, 738.

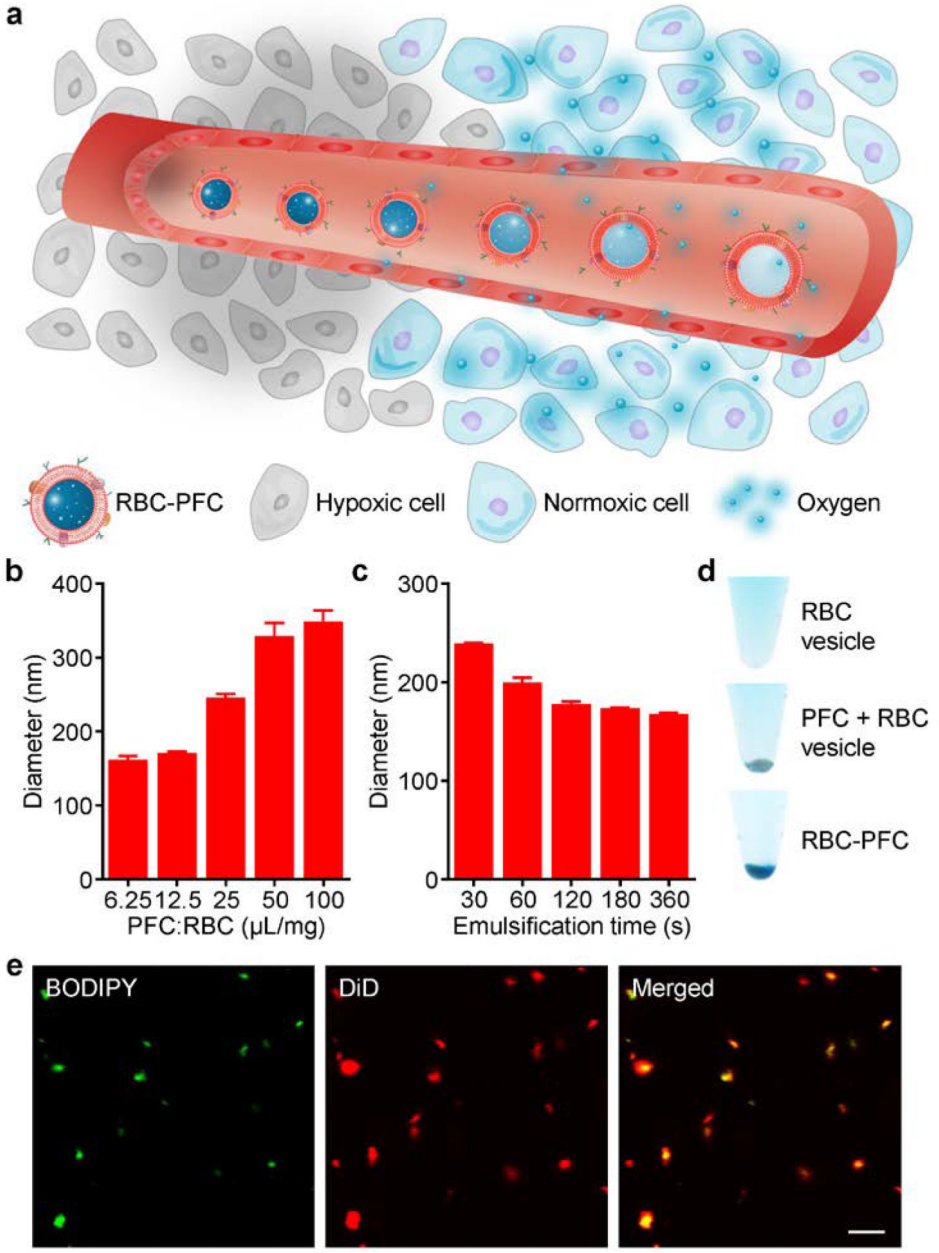

Figure 1.

Formulation of RBC-PFC. a) Schematic illustration of oxygen delivery and release to hypoxic tissues by RBC-PFC. b) Diameter of RBC-PFC at various PFC to RBC membrane ratios (n = 3, mean + s.d.). c) Diameter of RBC-PFC after various emulsification times (n = 3, mean + s.d.). d) Images of RBC membrane vesicles, bare PFC emulsions mixed with RBC vesicles, and RBC-PFC after centrifugation at 600*g*; the RBC membrane was labeled with DiD. e) Confocal fluorescence imaging of dual-labelled RBC-PFC; the RBC membrane was labelled with DiD (red), and the PFC core was labelled with BODIPY (green). Scale bar, 1 μm.

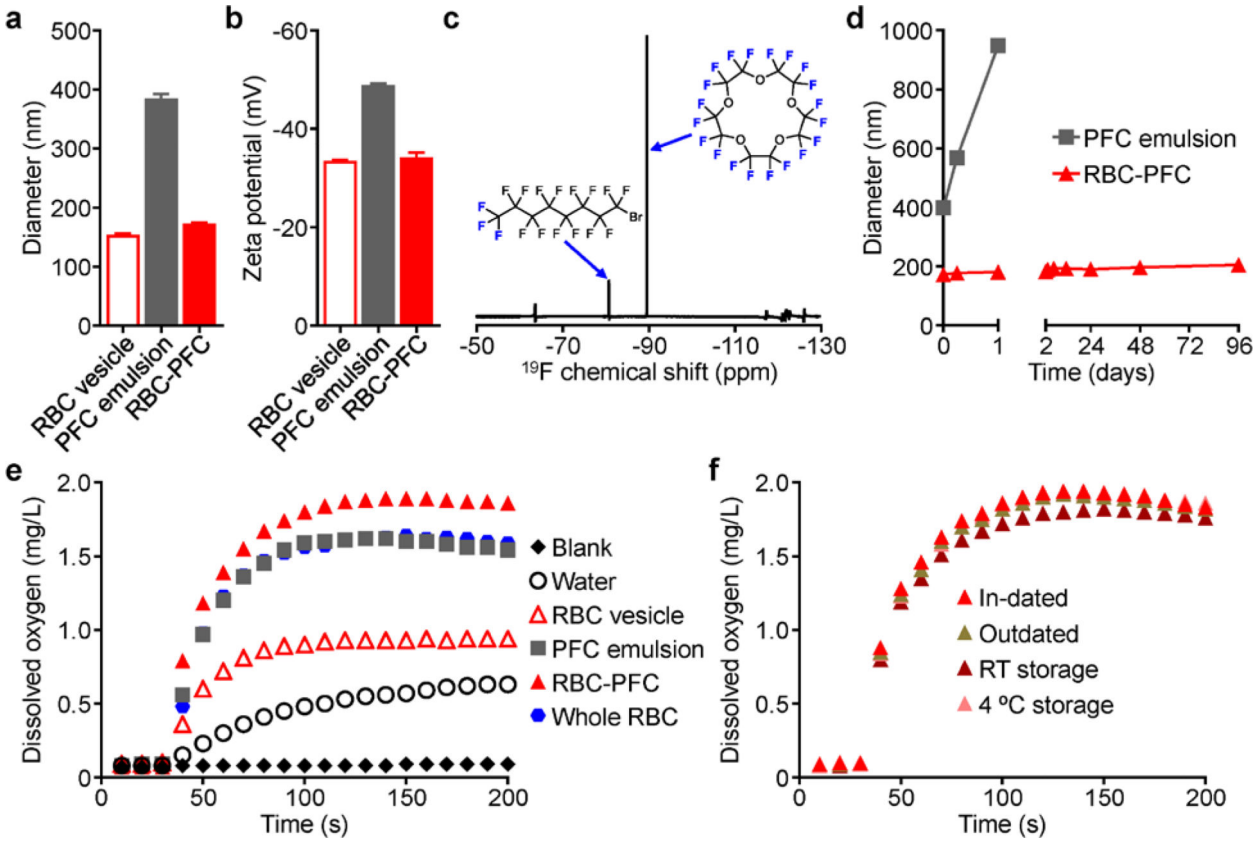

Figure 2.

RBC-PFC characterization. a) Diameter of RBC vesicles, bare PFC emulsions, and RBC-PFC (n = 3, mean + s.d.). b) Zeta potential of RBC vesicles, bare PFC emulsions, and RBC-PFC (n = 3, mean + s.d.). c) Quantification of perfluorooctyl bromide (left) loading by ^{19}F-NMR, where perfluoro-15-crown-5-ether (right) was used as an internal standard; the fluorine atoms corresponding to each respective peak are colored in blue. d) Stability of bare PFC emulsions and RBC-PFC over the course of 96 days (n = 3, mean ± s.d.). e) Dissolved oxygen kinetics after the addition of oxygenated water, RBC vesicles, PFC emulsions, RBC-PFC, or whole RBCs into deoxygenated water. f) Dissolved oxygen kinetics after the addition of RBC-PFC fabricated from in-dated or outdated human RBCs, as well as human RBC-PFC after storage for 1 week at either room temperature (RT) or 4 °C.

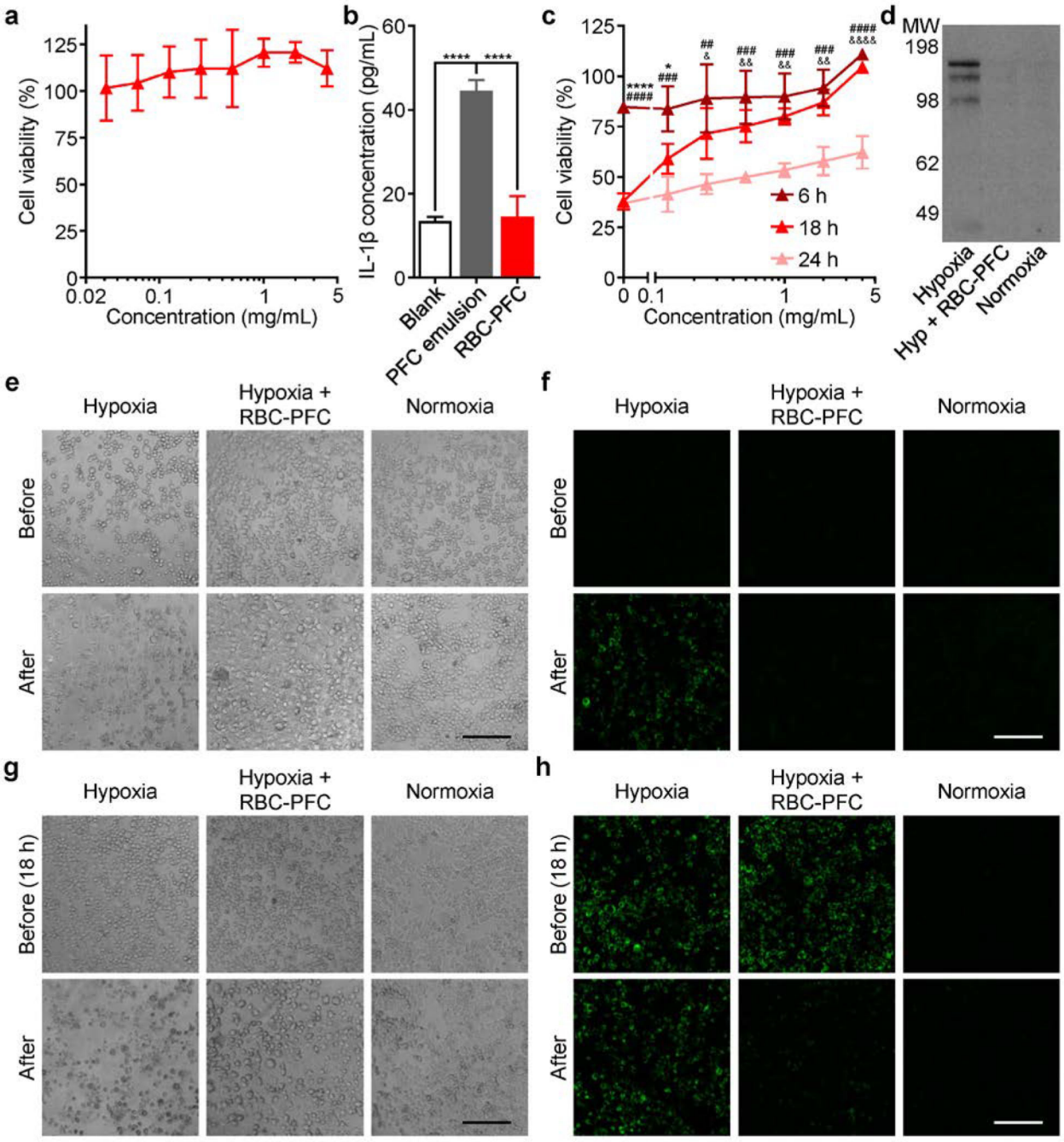

Figure 3.

In vitro oxygen delivery using RBC-PFC. a) Viability of Neuro2a cells after incubation with RBC-PFC at various concentrations for 24 h ($n = 6$; mean ± s.d.). b) Cytokine levels produced by J774 macrophages after incubation with PFC emulsions or RBC-PFC for 24 h ($n = 3$; mean + s.d.). ****$p < 0.0001$; one-way ANOVA. c) Viability of Neuro2a cells after different hypoxia induction periods, followed by incubation with RBC-PFC at various concentrations for 24 h under hypoxic conditions ($n = 6$; mean ± s.d.). *$p < 0.05$, ****$p <$ 0.0001 (6 h vs. 18 h); ##$p < 0.01$, ###$p < 0.001$, ####$p < 0.0001$ (6 h vs. 24 h); &$p < 0.05$,

&&$p < 0.01$, &&&&$p < 0.0001$ (18 h vs. 24 h); one-way ANOVA. d) Western blot for HIF1α expression in Neuro2a cells subject to hypoxia, hypoxia in the presence of RBC-PFC following an 18 h induction period, or normoxia. MW, molecular weight in kDa. e,g) Brightfield microscopy of Neuro2a cells before and 24 h after being subject to hypoxia, hypoxia in the presence of RBC-PFC, or normoxia; cells were subject to either 0 h (e) or 18 h (g) of hypoxia induction. Scale bars, 200 μm. f,h) Fluorescence microscopy of Neuro2a cells before and 6 h after being subject to hypoxia, hypoxia in the presence of RBC-PFC, or normoxia; cells were labeled with Image-iT Green hypoxia reagent (green) and were subject to either 0 h (f) or 18 h (h) of hypoxia induction. Scale bars, 200 μm.

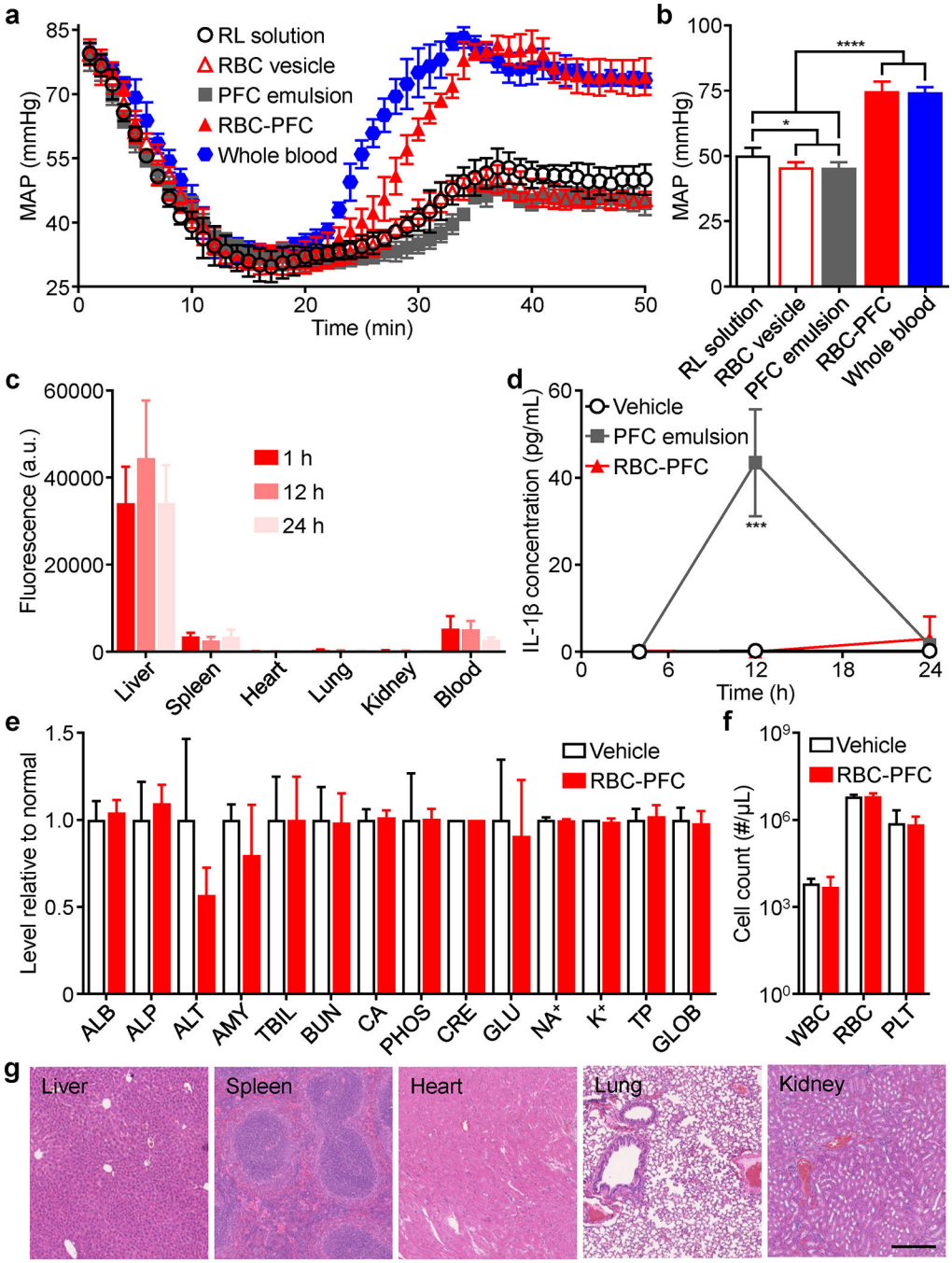

Figure 4.

In vivo oxygen delivery and safety of RBC-PFC. a) Mean arterial pressure (MAP) profiles of mice after blood withdrawal, followed by infusion with Ringer's lactate (RL), RBC vesicles, PFC emulsions, RBC-PFC, or whole blood ($n = 6$; mean ± s.d.). b) MAP values for each group at the endpoint of (a) ($n = 6$; mean + s.d.). *$p < 0.05$, ****$p < 0.0001$; one-way ANOVA. c) Biodistribution of DiD-labeled RBC-PFC in major organs, including the liver, spleen, heart, lungs, kidneys, and blood, at various times after administration ($n = 6$; mean + s.d.). d) Serum cytokine levels over time after intravenous administration of isotonic sucrose

(vehicle), PFC emulsions, or RBC-PFC (n = 3; mean ± s.d.). ***p < 0.001; one-way ANOVA. e) Comprehensive blood chemistry panel taken 24 h after intravenous administration of isotonic sucrose or RBC-PFC (n = 3; mean + s.d.). ALB: albumin, ALP: alkaline phosphatase, ALT: alanine transaminase, AMY: amylase, TBIL: total bilirubin, BUN: blood urea nitrogen, CA: calcium, PHOS: phosphorus, CRE: creatinine, GLU: glucose, NA^+: sodium, K^+: potassium, TP: total protein, GLOB: globulin (calculated). f) Counts of various blood cells 24 h after intravenous administration of isotonic sucrose or RBC-PFC (n = 3; geometric mean + s.d.). WBC: white blood cells, RBC: red blood cells, PLT: platelets. g) Hematoxylin and eosin (H&E) staining of histology sections from major organs 24 h after RBC-PFC administration. Scale bar, 250 μm.